Science of the Total Environment 703 (2020) 135475

Contents lists available at ScienceDirect

Science of the Total Environment

journal homepage: www.elsevier.com/locate/scitotenv

Ectomycorrhizal fungus-associated determinants jointly reflect ecological processes in a temperature broad-leaved mixed forest

Zhen Bai [a,1], Zuo-Qiang Yuan [a,1], Dong-Mei Wang [b], Shuai Fang [a], Ji Ye [a], Xu-Gao Wang [a,*], Hai-Sheng Yuan [a,*]

[a] CAS Key Laboratory of Forest Ecology and Management, Institute of Applied Ecology, Chinese Academy of Sciences, Shenyang 110164, PR China
[b] School of pharmacy, Shenyang Pharmaceutical University, 72 Wenhua Road, Shenyang 110016, PR China

HIGHLIGHTS

- Geographic, edaphic and floristic gradients are separately determined by composite scores.
- Tree and ECM fungal species show significant dissimilarities along environmental gradients.
- Environmental gradients interactively influence floristic and ECM fungal life strategies.
- ECM-associated determinants jointly reflect local-scale ecological processes.

GRAPHICAL ABSTRACT

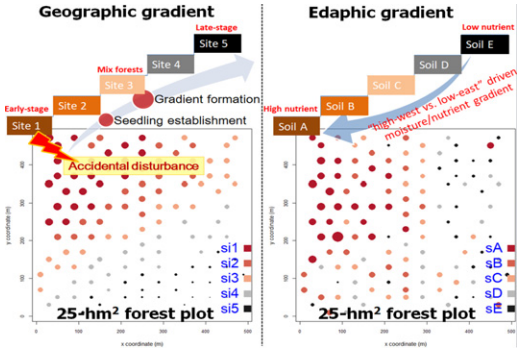

ARTICLE INFO

Article history:
Received 30 July 2019
Received in revised form 5 November 2019
Accepted 9 November 2019
Available online 14 November 2019

Editor: Elena Paoletti

Keywords:
Ectomycorrhizal (ECM) fungi
Broad-leaved mixed-forest
Environmental gradient
Plant functional trait
Soil nutrient
Geographical site

ABSTRACT

Ectomycorrhizal (ECM) fungi are closely related to vegetation compositions, edaphic properties, and site-specific processes. However, the coevolutionary mechanisms underlying the spatial distributions in floristic and ECM fungal composition in the context of biotic adaptations and abiotic variances remain unclear. We combine a total of 25 ECM fungus-associated environmental variables to impose three types of composite scores and then quantify the environmental gradients of geographical site, soil chemical property and vegetation functional trait across 122 grids of 20 m × 20 m in a 25-hm^2 forest plot. Significant dissimilarities in vegetational and ECM fungal abundance and composition existed along the above environmental gradients. Specifically, a contrasting floristic distribution (e.g., *Betula platyphylla* vs. *Tilia mandshurica*) existed between the northeastern and southwestern areas and was closely related to the nutrient and moisture gradients (with high levels in the west and low levels in the east). Furthermore, the ECM fungal communities were more abundant in the nutrient-poor and low-moisture environments than in the nutrient-rich and high-moisture environments, and the mixed-forest in the middle-gradient sites between the northeastern and southwestern areas harbored the highest ECM fungal diversity. These findings suggest that predictable within-site vegetation succession is closely related to ECM-associated determinants and the natural spatial heterogeneity of edaphic properties at a local scale.

© 2019 Elsevier B.V. All rights reserved.

* Corresponding authors.
E-mail addresses: wangxg@iae.ac.cn (X.-G. Wang), hsyuan@iae.ac.cn (H.-S. Yuan).
[1] These authors contributed equally.

https://doi.org/10.1016/j.scitotenv.2019.135475
0048-9697/© 2019 Elsevier B.V. All rights reserved.

1. Introduction

A total of 20,000–25,000 ectomycorrhizal (ECM) fungi species have been recognized globally, of which most belong to Basidiomycetes or Ascomycetes (Cairney, 2012; Kumar and Atri, 2017). Their mycelia can penetrate the root cortex to form a Hartig net and thereby facilitate nutrient and water acquisition by the host in exchange for photosynthetically derived carbon (C) compounds (Cairney, 2012; Kumar and Atri, 2017). Thus, ECM fungi serve as a primary nutrient gathering interface for their hosts by scavenging nitrogen (N), phosphorus (P), and trace elements from both inorganic and organic pools, resulting in a redistribution of nutrients from mineral and organic substrates to plant biomass (Cheeke et al., 2017; Craig et al., 2018; Horton and Bruns, 2001).

Accordingly, floristic morphology, nutrient status and ecological function are always closely related to ECM symbioses. For instance, ECM-dominated roots are consistently characteristic of high tissue density due to high proportions of lignified stele area (Valverde-Barrantes et al., 2018). Seedling foliar C/N ratios are negatively correlated with *Russula nitida*, which prefers to mobilize labile N resources for host plants (Hewitt et al., 2017). Though early-successional plant species present fewer links caused by fewer fungal partners than late-successional species (the latter allows for a lasting fungal recruitment) (Taudiere et al., 2015), early-established colonizers may provide secondary ones with compatible ECM fungal symbionts (Nara, 2006b).

Additionally, ECM fungal community composition and diversity can also change greatly due to direct influences of soil properties, such as moisture, pH, N, organic matter and potassium (K) (Aponte et al., 2010; Jarvis et al., 2015; Koizumi et al., 2018). ECM biomass and ECM root area linearly increase with soil C/N ratio, which suggests that host plants allocate more biomass to ECM-root absorptive surface area to increase the N uptake rate (Ostonen et al., 2011). Furthermore, the ECM genus *Rhizopogon* is closely related to low soil K concentrations, probably because ECM symbioses preferentially allocate nearby soil metals to fast-growing host seedlings (Wen et al., 2018).

Moreover, ECM fungal community structure does not differ between coexisting trees but is significantly dissimilar between geographical locations, which indicates infrequent ECM fungal migration over certain geological periods (Wen et al., 2015). The varying soil moisture along an altitudinal gradient of 300 m in the same forest stand can cause shifts in ECM fungal composition (Jarvis et al., 2015). Certain mycorrhizae are even patchily distributed across a 20 m × 20 m plot, due to underlying root morphology, mycorrhizal functions, and consistent interspecific interactions within the ECM fungal community (Pickles et al., 2010).

Collectively, the ECM fungal community richness and composition are interactively influenced by host plants and abiotic variables (Matsuoka et al., 2016; Obase et al., 2009; Ruotsalainen et al., 2009), especially in terms of early-stage vs. late-stage vegetation composition (Clemmensen et al., 2015), soil chemical properties (Kumar and Atri, 2017) and geographical parameters (Matsuoka et al., 2016; Põlme et al., 2013). These ECM fungus-associated determinants are separately controlled by vegetation life histories, soil nutritional statuses, and site-specific processes (Condit et al., 2013; Põlme et al., 2013; Ruotsalainen et al., 2009; Toljander et al., 2006). Hence, we hypothesized that 1) ECM-associated variables would present spatial distribution patterns or environmental gradients due to biotic adaptations and abiotic variances, 2) such gradients could be imposed by composite scores derived from geological site, soil nutritional status and vegetation functional trait, respectively, and 3) these obtained gradients would in turn explain distinct biotic adaptations to specific abiotic variances during vegetation-ECM successional processes at a local scale. By combining data on ECM fungal community composition and diversity, plant species abundance, floristic functional trait, soil nutritional status and geological parameter, we aimed to 1) reveal the shifts in floristic and ECM fungal composition in the context of biotic adaptations and abiotic variances; and 2) identify the coevolutionary mechanisms underlying the vegetation-ECM spatial distribution driven by site-specific environmental variables.

2. Materials and methods

2.1. Forest plot (25 hm^2)

In 2004, a 25-hm^2 (500 × 500 m) plot was established in the core zone of a broad-leaved Korean pine mixed-forest in the Changbai Mountain Natural Reserve (CMNR) of northeastern China (42°23′ N,128°05′E) (Hao et al., 2007; Yuan et al., 2016). The mean annual precipitation is approximately 700 mm, and most of this precipitation occurs from June to September (480–500 mm). The mean annual temperature is 2.8 °C, the January mean temperature is −13.7 °C and the July mean temperature is 19.63 °C. The mean canopy tree age is approximately 280 years. Natural disturbances occur due to strong wind in spring and winter. According to topographic attributes (elevation and slope), the 25-hm^2 plot can be classified as a low plateau in the western half (slope < 7°, elevation < 804 m) and a high plateau in the eastern half (slope < 7°, elevation ≥ 804 m). Due to water transport from the higher plateau to the lower plateau, significantly higher soil moisture occurs on the low plateau (Yuan et al., 2016). All free-standing woody stems ≥1 cm in trunk diameter were mapped, measured and identified to the species level. The first census in July 2004 found 36,908 individuals belonging to 52 species, 32 genera and 18 families, whereas a survey in 2014 found 34,926 individuals belonging to 51 species. The plant species include four vertical layers (Yuan et al., 2012): (1) dominant competitor: *Pinus koraiensis*; (2) canopy layer: *Ulmus japonica*, *Quercus mongolica*, *Tilia mandshurica*; (3) subcanopy layer: *Acer mono*, *Betula platyphylla*, *Ulmus laciniata*, *Maackia amurensis*, *Acer pseudosiebodianum*, *Syringa reticulata*; and (4) shrub layer: *Acer barbinerve*. The stand soil is affiliated with dark brown forest soil (mollisol according to the U.S. Soil Taxonomy Series, 1999).

2.2. Soil collection

The 25-hm^2 plot was divided into 625 nonoverlapping 20 m × 20 m grids (quadrats). In August 2017, we collected soil samples from 150 grids with seed traps; the grids were chosen with systematic regular pattern (Fig. S1). A total of 21 grids were excluded to avoid edge effects or large belowground roots. Thus, 129 soil samples were used for further data analysis. A composite soil sample representing each 20 m × 20 m grid was created by thoroughly mixing five soil cores collected from the grid at depths of 0–10 cm. The soil samples were transported at 4 °C, freshly sieved (< 2 mm) and either stored at −80 °C for DNA extraction or air-dried for chemical variable analyses.

2.3. Environmental variables

With the methods previously reported (Yuan et al., 2012), the longitude (x) and latitude (y) coordinates and elevation (meanelev) measurements of each sample were recorded as geographical data; and the soil chemical properties, including soil organic matter (SOM), available N (AN), available P (AP), available K (AK), pH, and water content (WC), were also measured. Plant diversity (i.e., taxonomic, phylogenetic and functional), functional identity and stand structural attribute data were used to represent the multiple biotic predictors in each 20 m × 20 m quadrat. Taxonomic diversity was calculated using four widely used phylogenetic diversity indexes, i.e., Faith's phylogenetic diversity (PD), mean nearest taxon distance (mntd), phylogenetic species variability (psv) and evenness (E), via the Phylomatic informatics tool (http://www.phylodiversity.net) based on the updated time-calibrated branch length of seed plants with multigene molecular and fossil data (Zanne et al., 2014). Functional diversity was assessed by functional dispersion diversity (FD) based on four key traits, i.e., the specific leaf area (FD.sla), leaf phosphorus content (FD.lpc), leaf nitrogen

content (FD.lnc) and maximum tree height (FD.H) (Laliberté and Legendre, 2010). We selected leaf area (LA), leaf nitrogen content (LNC), wood specific gravity (WSG) and specific root length (SRL) to determine the functional identity of the most dominant species (Grime, 1998). We quantified the stand structural attributes by calculating Shannon-Wiener diversity indexes based on basal areas or diameters at breast height (DBH). Specifically, within each 20 m × 20 m quadrat, the index of ssd.ba.4 was derived by the relative proportions of basal area for a given DBH discrete class (i.e., 4 cm) (Bourdier et al., 2016); the index of ssd.8 was calculated based on the proportions of tree DBH classes for a given discrete DBH (i.e., 8 cm) (Ali et al., 2016). In addition, the average aboveground biomass of three forest inventories (mean) and stem density (ind) were further included as proxies of community structure.

2.4. DNA extraction and molecular analyses

Soil genomic DNA was extracted with 0.25 g of a soil sample using the MoBio PowerSoil® DNA Isolation extraction kit (MoBio, California, USA). The DNA quality assessment was based on 260/280 nm and 260/230 nm absorbance ratios obtained with a NanoDrop Life Spectrophotometer (NanoDrop, Wilmington, USA). The final DNA was stored at −40 °C until use. The Internal Transcribed Spacer 1 (ITS1) region of ribosomal RNA gene cluster was amplified using the barcoded fusion primers 1737F (5′-GGAAGTAAAAGTCGTAACAAGG-3′) and 2043R (5′-ATGCAGGCTGCGTTCTTCATCGATGC-3′) (Zhang et al., 2016). Polymerase chain reaction (PCR) was carried out with a Gene Amp PCR-System 9700 (Applied Biosystems, Foster City, USA). PCR was performed in triplicate in a 20 μL mixture containing 4 μL of 5 × FastPfu buffer, 2 μL of 2.5 mM dNTPs, 0.8 μL of each primer (5 μM), 0.4 μL of FastPfu polymerase and 10 ng of template DNA. Thermal cycling conditions were as follows: initial denaturation step at 95 °C for 3 min; followed by 35 cycles at 95 °C for 30 s, annealing at 55 °C for 30 s and extension at 72 °C for 45 s; and a final extension at 72 °C for 10 min. The amplified ITS sequencing was performed with 300PE MiSeq (Illumina, San Diego, USA) at Shanghai Majorbio Biopharm Biotechnology Co., Ltd. (Shanghai, China).

2.5. Bioinformatic analyses

The data processing was carried out using QIIME (version 1.7) (http://qiime.org/tutorials/tutorial.html). All sequence reads were trimmed and assigned to each sample based on their barcodes. High-quality sequences (length > 200 bp, without ambiguous bases ("N"), and above average base quality score (> 25)) were used for the downstream analysis. Sequences were clustered into operational taxonomic units (OTUs) using UPARSE (version 7.1, http://drive5.com/uparse/) at a 97% threshold pairwise identity. Singletons and doubletons were removed during OTUs selection. The aligned ITS gene sequences were used for a chimera check using the UCHIME algorithm. Each sample was subsampled to a depth of 28,881 reads using the script *obisample*. The fungal OTUs were assigned to specific ECM fungi on the basis of FUNGuild (Nguyen et al., 2016). Alpha-diversity analyses (e.g., Shannon, Simpson, Inver_Simpson and Evenness) were performed by running a workflow on QIIME (the script "*core_diversity_analyses.py*"). Sequences were deposited in NCBI Sequence Read Archive under accession number PRJNA587220.

2.6. Statistical analyses

2.6.1. Multivariate analysis

An initial detrended correspondence analysis (DCA) in R (version 3.5.0) was applied to the OTU relative abundances and the environmental variables. The first axis length of the main DCA gradient was 4.47, which indicates a unimodal relationship between the taxa and environmental variables. Subsequently, a canonical correspondence analysis (CCA) was applied to the ECM fungal species that occurred in at least 10 plots or that had relative abundances >1%. Thus, a total of 488 species (out of 1218 ECM species) were used in the CCA (Fig. 1). Of 129 samples, seven samples were outliners in CCA patterns and thus 122 samples were finally used. Many unrelated individual variables would mask the signature of significant variables in Mantel tests and redundant variables could generate inaccurate and inefficient CCA models, hence the variance inflation factor (VIF) was used to maintain a reduced but representative sets of environmental and plant variables important to microbial community composition (He et al., 2010; Jagodziński et al., 2018). The variables with VIF values larger than 10 were removed, as they are strongly dependent on others and do not have independent information (Ali et al., 2017; Tuomisto et al., 2019). The fungal species (65 in total) with CCA1 and CCA2 scores larger than 1 or less than −1 were strongly associated with environmental variables and thus were presented in the CCA plot. The proportion of constrained inertia in the CCA accounted for 35.82% of the total inertia (explaining 35.82% of the variance structuring ECM fungal communities), and CCA1 and CCA2 accounted for 5.60% and 5.44% of the constrained inertia, respectively (Fig. 1).

2.6.2. Site_Gr, soil_Gr and plant_Gr

According to the CCA (Fig. 1), at least three types of variables significantly or marginally influenced the ECM fungal community composition: geographical sites (in red), plant function indexes (in green), and soil chemical properties (in blue). To conduct a global assessment of spatially explicit grading patterns of geographical sites, plant functions and soil nutrients in 122 grids, we calculated composite scores by combining the key variables of each environmental type. For the composite scores of the geographical sites (i.e., site_score), we first scaled the x, y and meanelev. Then, the means of the scaled x, y and meanelev data of each plot were calculated, and the composite scores of geographical site were obtained. The site_score values were derived from positive values of meanelev and y and negative values of x because meanelev and y were positively related to soil properties whereas negative correlations were observed between x and soil nutrients (Fig. 1, S2). Variables that were positively related to soil properties and contributed to the composite scores of plant functional indexes (i.e., plant_score) included SRL, LNC, LA, WSG and ssd.ba.4, whereas those with negative contributions to plant_score included FD.lpc FD.H, E, ssd.8 and mean (Fig. 1, S2). The soil variables all positively contributed to the composite scores of soil nutrient (i.e., soil_score). The above-mentioned variables were not weighted mainly because 1) their positive or negative contributions to composite scores were partially based upon their correlations with soil properties (Fig. S2); and 2) their relationships could vary between CCA of ECM fungal communities (Fig. 1) and direct correlation analyses (Fig. S2). Using "quantile" at 0.8, 0.6, 0.4 and 0.2, we graded site_score at five gradient levels (site_Gr): si1, scores were > 0.8; si2, scores were between 0.6 and 0.8; si3, scores were between 0.4 and 0.6; si4, scores were between 0.2 and 0.4; and si5, scores were < 0.2. Thus, the 122 grids were distributed from northwest (site1) to southeast (site5) (Fig. S1). Similarly, soil gradients (soil_Gr) were imposed from west to east and included sA, sB, sC, sD and sE; and plant gradients (plant_Gr) were imposed at pA, pB, pC, pD and pE (Fig. S1). This simple and clear five-gradient scheme is widely used in academic research (Nabiollahi et al., 2018), which presents the explicit local-scale differentiation of ECM fungus-associated determinants associated to geographical sites, plant functions and soil nutrients, respectively.

2.6.3. Correlation and nonparametric analyses

The geographical parameters, soil chemical properties and plant functional indexes were all normalized to obtain a mean of 0 and a standard deviation of 1 before the analyses. Corrplot and Kendall correlations and multivariate analyses (ADONIS) were carried out in R to reveal the relationships among variables as well as their interaction effects on the beta-diversity of ECM communities. Because the

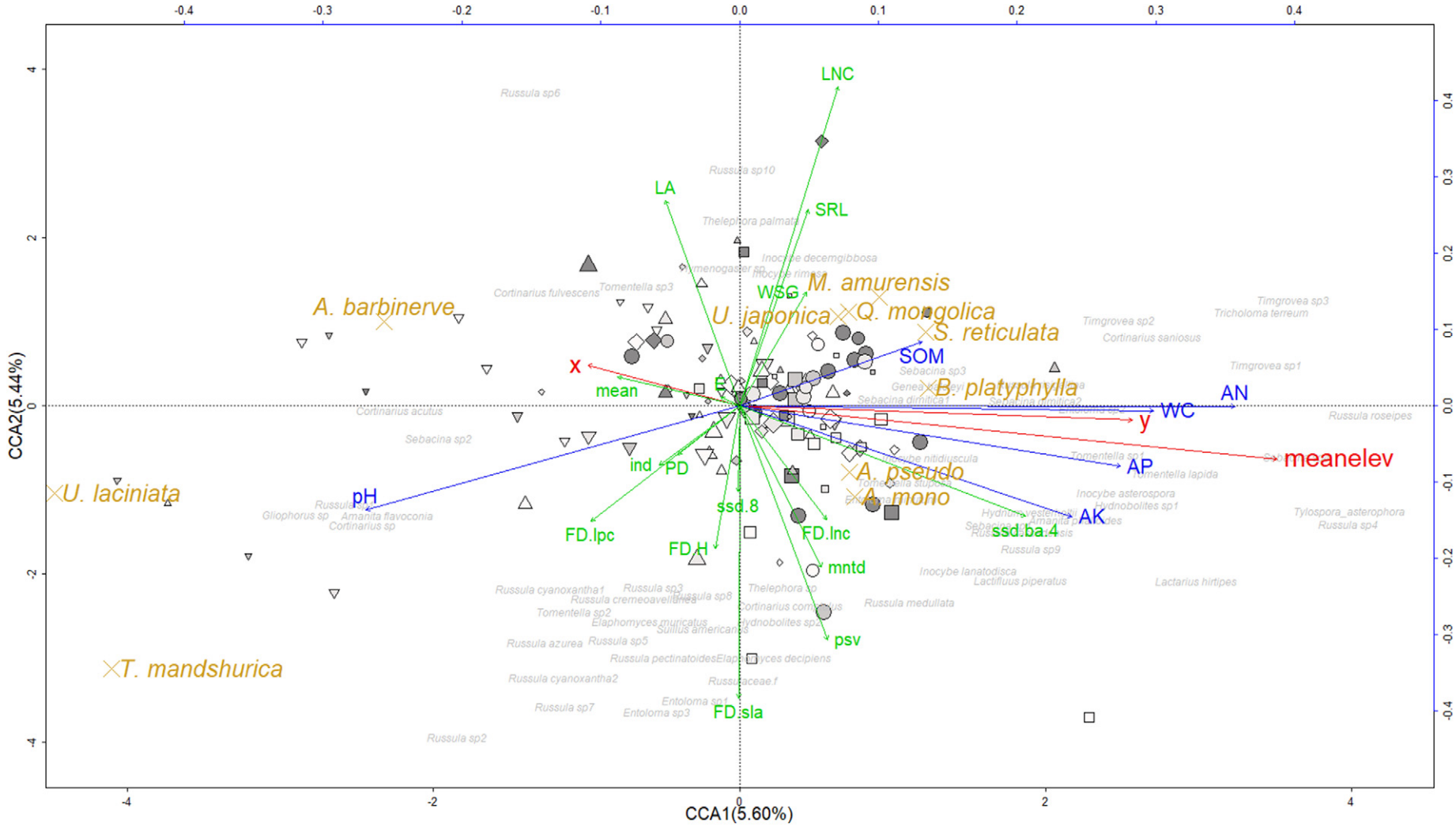

Fig. 1. Canonical correspondence analysis (CCA) of ECM fungal communities. The geographical gradients are separately represented by solid circles (si1), solid squares (si2), solid diamonds (si3), solid triangles pointing upward (si4) and solid triangles pointing downward (si5). The soil nutrient gradients are indicated by dot size and ranked from large to small as sA (cex = 3), sB (cex = 2.5), sC (cex = 2), sD (cex = 1.5) and sE (cex = 1). Vegetation gradients are represented as Snow4 (pA), Snow3 (pB), Snow2 (pC), Snow1 (pD) and Snow (pE). The geographical parameters (in red) include longitude (x), latitude (y), and elevation (meanelev). Vegetation functional traits (in green) include leaf area (LA), leaf nitrogen content (LNC), wood density (WSG), average above-ground biomass (mean), stem density (ind) and specific root length (SRL), specific leaf area (FD.sla), leaf phosphorus content (FD.lpc), leaf nitrogen content (FD.lnc) and maximum tree height (FD.H), phylogenetic species variability (psv), Faith's phylogenetic diversity (PD), mean nearest taxon distance (mntd), community structure diversity indexes separately based on average diameter at breast height of 4 cm (ssd.ba.4) and 8 cm (ssd.8), and evenness (E). Soil chemical properties (in blue) include soil organic matter (SOM), water content (WC), pH, available N (AN), available P (AP) and available K (AK). Tree species (in gold) are denoted by *U.japonica* (*Ulmus japonica*), *Q.mongolica* (*Quercus mongolica*), *T.mandshurica* (*Tilia mandshurica*), *A.mono* (*Acer mono*), *B.platyphylla* (*Betula platyphylla*), *U.laciniata* (*Ulmus laciniata*), *M.amurensis* (*Maackia amurensis*), *A.pseudo* (*Acer pseudosiebodianum*), *S.reticulata* (*Syringa reticulata*) and *A.barbinerve* (*Acer barbinerve*).

assumption of variance homogeneity could not be met, nonparametric analyses (Kruskal-Wallis test) were conducted with Statistica 10 (StatSoft Inc., Tulsa, USA) to determine whether the vegetation and ECM fungal communities varied significantly across three categories of environmental gradients, i.e., Site_Gr, soil_Gr and plant_Gr.

3. Results

3.1. Environmental variables, composite scores and gradients

The CCA showed that the ECM fungal community structure was fundamentally influenced by three kinds of environmental variables (25 variables in total), including geographical parameters (i.e., "site", red arrows), soil chemical properties (i.e., "soil", blue arrows) and plant functional indexes (i.e., "plant", green arrows) (Fig. 1). The variables were distributed in opposite directions either along the CCA1 axis (e.g., geographical parameters "y", "meanelev" vs. "x") or along the CCA2 axis (e.g., plant indexes "LNC", "SRL" and "LA" vs. "FD.sla" and "psv") (Fig. 1).

To precisely visualize the driving forces associated with distinct environmental variances, the site-, soil- and plant-associated variables were separately combined to calculate the composite scores (i.e., site_score, soil_score and plant_score), and thereafter, environmental gradients were imposed at five levels (i.e., site_Gr, soil_Gr and plant_Gr) (see "Statistical analyses" and Fig. S1). Across the 25-hm^2 forest plot, the environmental gradients were clearly presented as follows: 1) the site_score values ranked higher in the northwestern part (e.g., si1 in brown) than in the southeastern part (e.g., si5 in black), and 2) soil_score values were higher in the western part (e.g., sA in brown) than in the eastern part (e.g., sE in black) (Fig. S1). The abovementioned three composite scores were strongly and positively correlated with each other based on Kendall's (tau) correlation (Fig. 2).

3.2. Vegetation communities along the environmental gradients

A total of 10 vegetation species were observed to significantly influence ECM fungal composition and were separated into contrasting groups either along the CCA1 axis (e.g., *Ulmus laciniata* vs. *Betula platyphylla*) or along the CCA2 axis (e.g., *Maackia amurensis* vs. *Acer mono*) (Fig. 1). The three composite scores showed strong correlations with the abundances of the plant species either positively (e.g., *Betula platyphylla* and *Syringa reticulata*) or negatively (e.g., *Ulmus laciniata*, *Tilia mandshurica* and *Acer barbinerve*) ($P < .05$; Fig. 2). Furthermore, the abundances of different vegetation species exhibited contrasting trends along five quality gradients of site_Gr, soil_Gr and plant_Gr (Table 1). For instance, *Betula platyphylla* existed in site1 but not in site5; the opposite was true for *Ulmus laciniata* and *Tilia mandshurica*. Moreover, *Betula platyphylla* was not encountered at the low soil nutrient status (e.g., sD and sE); in contrast, *Tilia mandshurica* and *Ulmus laciniata* did not exist at the high soil nutrient status (e.g., sA and sB).

3.3. ECM fungal communities along the environmental gradients

A total of 1218 ECM fungal species were found in the 25-hm^2 forest plot. The ECM fungal community compositions along the environmental gradients were predominantly influenced by 65 species, as the absolute values of their CCA1 or CCA2 scores were > 1. Among them, approximately 60 species were affiliated with Basidiomycota, and only five were affiliated with Ascomycota. These ECM fungal species (except for *Russula risigallina* and *Hydnobolites* sp1) were clustered into 15 key groups (KeyG) based on a global Kendall W test and mean Spearman correlation coefficients of the individual species in each group (Table S1).

The ADONIS showed significant differences ($P < .01$) in the ECM fungal community composition along five environmental gradients of site_Gr ($R^2 = 0.053$), soil_Gr ($R^2 = 0.040$) and plant_Gr ($R^2 = 0.039$) (Table S2). These results indicated that site_Gr, soil_Gr and plant_Gr at most explained 5.3, 4.0 and 3.9% of the variance, respectively, in the ECM fungal communities encountered across this 25-hm^2 forest plot. Additionally, according to the non-parametric Kruskal-Wallis tests (Table 2), the ECM fungal abundance (%) was marginally affected by site_Gr ($P = .133$) or significantly influenced by plant_Gr ($P = .024$) and soil_Gr ($P = .004$). The three composite scores showed significant and negative correlations with cumulative number of ECM fungal species (S.cum) ($P < .05$) (Fig. 2).

3.3.1. Soil_Gr

The relative abundances and S.cum of ECM fungi significantly increased from the higher nutrient status (e.g., sA) to the lower status (e.g., sE) (Table 2) and either increased by 0.60-fold from ca. 34% to ca. 54% or by 0.16-fold from ca. 126 to ca. 146 per grid (20 m × 20 m). Similarly, significant increases occurred with KeyG2 (from sA (0.002 ± 0.001) to sE (1.308 ± 0.873)) and KeyG13 (from sA/sB (0.001 ± 0.001) to sD (0.003 ± 0.001)) (Table 3). Additionally, significant negative correlations occurred between soil chemical properties (e.g., WC, SOM and AN) and most of the 65 key species except for some from KeyG8 and KeyG11 (Fig. 3).

3.3.2. Site_Gr

Interestingly, the highest relative abundances and S.cum of the ECM fungal communities occurred in the middle sites, i.e., ECM fungal abundances peaked at site2 and site3 (ca. 50%) ($P = .133$); cumulative species peaked at site3 (ca. 149 per grid) ($P = .009$) (Table 2). Similarly, the middle sites also had the highest relative abundances of KeyG9 (ca.1.9% at si3, $P < .001$) (Table 3). Moreover, strong site_Gr effects occurred with the relative abundances of KeyG2, KeyG5, KeyG13 and KeyG15, which increased ca. 558-, 10-, 8- and 103-fold from si1 to si5, respectively (Table 3). In particular, significant positive correlations were observed between the longitude (x) and the ECM fungal species from KeyG2, KeyG5, KeyG13 and KeyG15 (Fig. 3).

3.3.3. Plant_Gr

Significant effects of plant_Gr were observed for the total ECM fungal abundance (%), which was highest at pB (52.350 ± 5.002) and lowest at pC (33.063 ± 4.213) ($P < .05$; Table 2), or for KeyG8, which marginally decreased from pA (0.057 ± 0.048) to pE (0.005 ± 0.004) (Table 3). Moreover, significant positive correlations were observed between *Ulmus laciniata* and *Tilia mandshurica* and the ECM fungal species from KeyG2, KeyG14 and KeyG15 (Fig. 3).

4. Discussion

4.1. Closely-related environmental gradients

4.1.1. Soil and site interaction

All soil nutrients were positively related to latitude (y) but negatively related to longitude (x) (Fig. 1, Fig. S2), and large variation in soil chemical properties was explained by geographical parameters (Fig. 2). Our previous study similarly showed that over 70% of the variation in soil organic C density was explained by the coordinates (Yuan et al., 2013). Such an extremely significant correlation between soil chemical properties and geographical parameters has also been observed previously (Toljander et al., 2006).

In fact, the current 25-hm^2 forest plot could be subdivided into low plateau (nearly half of the area is in the western part, elevation< 804.0 m) and high plateau (nearly half of the area is in the eastern part, elevation ≥ 804.0 m) (Yuan et al., 2016). This topographic difference can cause surface transport of water and thus significantly higher soil moisture in the lower western plateau than the higher eastern plateau. During the transportation processes, soil nutrients are likely leached from the higher (east) to lower (west) plateau.

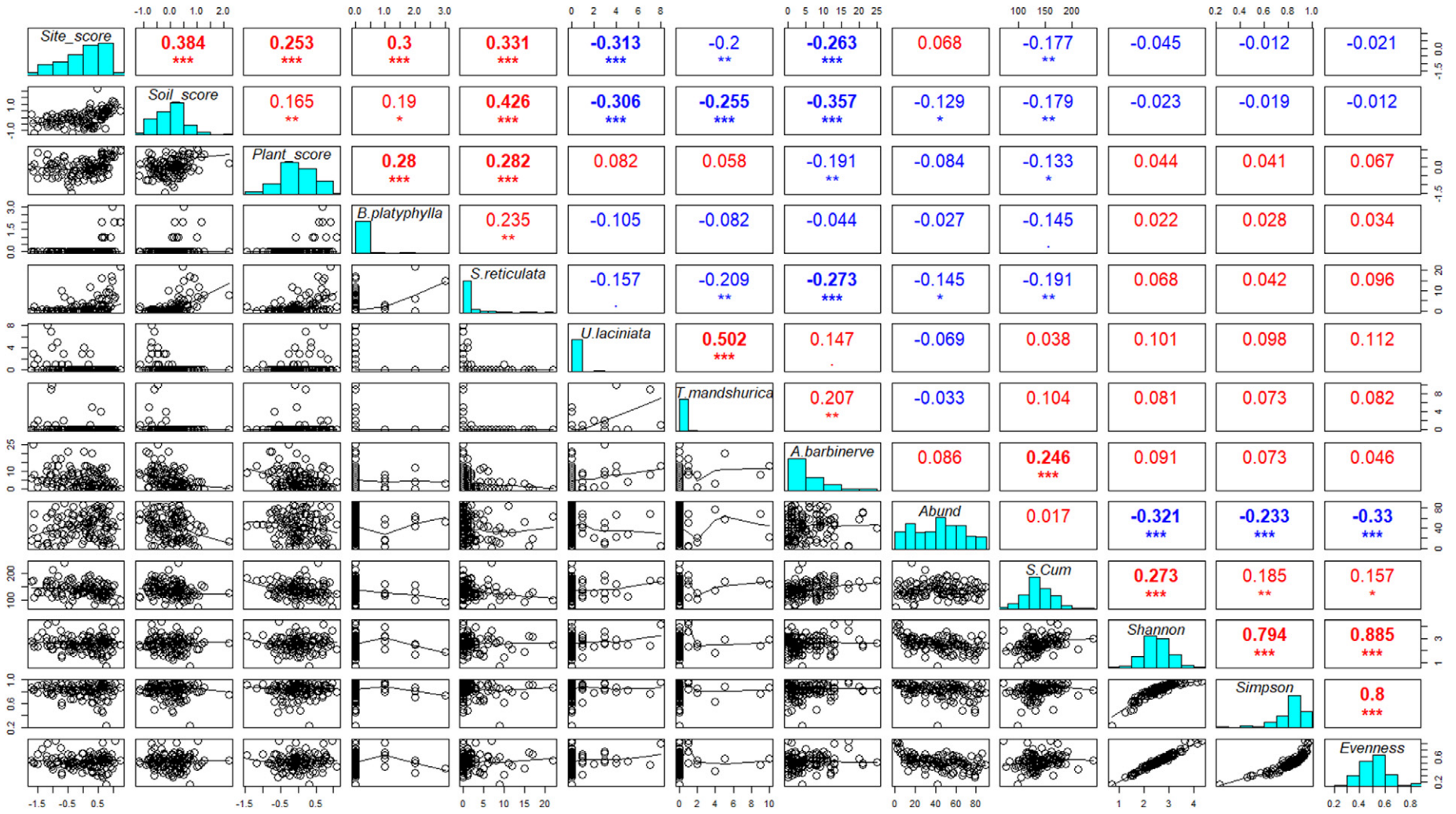

Fig. 2. Multipanel display of pairwise relationships between the composite scores and key vegetation species and ECM fungal diversity with Kendall tau rank correlations. Kendall correlations are applied with R. The composite scores include geographic parameters (Site_score), soil chemical properties (Soil_score) and vegetation function traits (Plant_score). Key tree species are denoted by *B.platyphylla* (*Betula platyphylla*), *S.reticulata* (*Syringa reticulata*), *U.laciniata* (*Ulmus laciniata*), *T.mandshurica* (*Tilia mandshurica*) and *A.barbinerve* (*Acer barbinerve*). ECM fungal abundance and richness indexes are indicated as Abund (abundance), S.Cum (cumulative numbers), Shannon (shannon wiener), Simpson and Evenness (evenness pielou). Kendall correlation coefficients are presented in red (positive) and in blue (negative), respectively. ***, $P < .001$; **, $P < .01$; *, $P < .05$.

Table 1
Key plant species abundances as affected by environmental gradients. Using "quantile" and grade score divisions at 0.8, 0.6, 0.4, and 0.2, we obtain five gradients of geographical site according to site_score: si1, scores > 0.8; si2, scores between 0.6 and 0.8; si3, scores between 0.4 and 0.6; si4, scores between 0.2 and 0.4; si5, scores < 0.2. Thus, plots from site1 to site5 separately distribute from northwest to southeast. Similarly, we establish five gradients of soil nutrient (soil_Gr), comprising sA, sB, sC, sD and sE, and five gradients of plant function index (plant_Gr), comprising pA, pB, pC, pD and pE. The abundances of key tree species (mean ± SE, standard error) at different environmental gradient levels are given in parentheses. Different letters between environmental gradients indicate significant differences at the P < .05 significance level as determined by nonparametric analyses (Kruskal-Wallis test) in Statistica 10 (StatSoft Inc., Tulsa, Okla., USA).

Tree species	Gr_site	Gr_plant	Gr_soil
Ulmus japonica	H (4, N = 122) = 14.732, P = .005	H (4, N = 122) = 14.140, P = .007	H (4, N = 122) = 17.467, P = .002
	si1 (2.880 ± 0.380) a	pA (3.120 ± 0.452) a	sA (3.240 ± 0.437) a
	si2 (1.792 ± 0.408) ab	pB (1.292 ± 0.252) b	sB (1.625 ± 0.329) b
	si3 (1.708 ± 0.327) ab	pC (1.625 ± 0.317) ab	sC (1.333 ± 0.274) b
	si4 (1.333 ± 0.280) b	pD (1.583 ± 0.361) b	sD (1.375 ± 0.268) b
	si5 (1.120 ± 0.279) b	pE (1.200 ± 0.216) b	sE (1.240 ± 0.284) b
Betula platyphylla	H (4, N = 122) = 21.199, P < .001	H (4, N = 122) = 28.349, P < .001	H (4, N = 122) = 7.691, P = .104
	si1 (0.440 ± 0.164) a	pA (0.520 ± 0.174) a	sA (0.320 ± 0.160) a
	si2 (0.125 ± 0.092) a	pB (ND)	sB (0.083 ± 0.058) a
	si3 (ND)	pC (0.042 ± 0.042) a	sC (0.167 ± 0.098) a
	si4 (ND)	pD (ND)	sD (ND)
	si5 (ND)	pE (ND)	sE (ND)
Acer mono	H (4, N = 122) = 27.187, P < .001	H (4, N = 122) = 8.203, P = .084	H (4, N = 122) = 35.786, P < .001
	si1 (19.560 ± 2.302) a	pA (16.720 ± 2.461) a	sA (18.040 ± 2.162) a
	si2 (10.292 ± 1.430) b	pB (10.333 ± 1.744) a	sB (12.292 ± 1.827) ab
	si3 (7.500 ± 1.107) b	pC (8.125 ± 1.200) a	sC (9.917 ± 1.277) b
	si4 (7.542 ± 0.903) b	pD (8.250 ± 0.875) a	sD (5.250 ± 0.578) c
	si5 (6.800 ± 0.922) b	pE (8.320 ± 1.220) a	sE (6.280 ± 0.838) bc
Syringa reticulata	H (4, N = 122) = 24.056, P < .001	H (4, N = 122) = 22.273, P < .001	H (4, N = 122) = 39.764, P < .001
	si1 (5.200 ± 1.178) a	pA (5.800 ± 1.232) a	sA (6.440 ± 1.204) a
	si2 (2.250 ± 0.752) ab	pB (1.542 ± 0.548) b	sB (2.167 ± 0.541) ab
	si3 (1.375 ± 0.524) b	pC (1.250 ± 0.439) b	sC (1.083 ± 0.442) bc
	si4 (1.375 ± 0.521) b	pD (1.208 ± 0.500) b	sD (0.375 ± 0.145) c
	si5 (0.320 ± 0.111) b	pE (0.680 ± 0.263) b	sE (0.400 ± 0.115) bc
Maackia amurensis	H (4, N = 122) = 37.522, P < .001	H (4, N = 122) = 15.964, P = .003	H (4, N = 122) = 24.368, P < .001
	si1 (1.480 ± 0.232) a	pA (1.240 ± 0.284) a	sA (1.280 ± 0.286) a
	si2 (0.917 ± 0.294) ab	pB (0.625 ± 0.215) ab	sB (1.083 ± 0.262) ab
	si3 (0.250 ± 0.173) b	pC (0.750 ± 0.257) ab	sC (0.417 ± 0.190) bc
	si4 (0.167 ± 0.098) b	pD (0.458 ± 0.159) ab	sD (0.083 ± 0.058) c
	si5 (0.320 ± 0.138) b	pE (0.080 ± 0.055) b	sE (0.280 ± 0.123) bc
Quercus mongolica	H (4, N = 122) = 14.377, P = .006	H (4, N = 122) = 28.026, P < .001	H (4, N = 122) = 5.031, P = .284
	si1 (1.920 ± 0.230) a	pA (1.680 ± 0.229) ab	sA (1.560 ± 0.265) a
	si2 (1.292 ± 0.259) ab	pB (2.250 ± 0.326) a	sB (1.208 ± 0.225) a
	si3 (0.833 ± 0.187) b	pC (1.042 ± 0.195) bc	sC (1.083 ± 0.232) a
	si4 (1.167 ± 0.231) ab	pD (0.917 ± 0.190) bc	sD (1.083 ± 0.288) a
	si5 (1.240 ± 0.307) ab	pE (0.600 ± 0.163) c	sE (1.520 ± 0.252) a
Ulmus laciniata	H (4, N = 122) = 19.447, P < .001	H (4, N = 122) = 2.282, P = .684	H (4, N = 122) = 16.899, P = .002
	si1 (ND)	pA (0.520 ± 0.342) a	sA (ND)
	si2 (ND)	pB (0.833 ± 0.389) a	sB (ND)
	si3 (0.458 ± 0.233) a	pC (0.333 ± 0.206) a	sC (0.208 ± 0.134) a
	si4 (0.208 ± 0.134) a	pD (0.208 ± 0.134) a	sD (0.500 ± 0.233) a
	si5 (1.280 ± 0.464) a	pE (0.080 ± 0.055) a	sE (1.240 ± 0.466) a
Tilia mandshurica	H (4, N = 122) = 11.351, P = .023	H (4, N = 122) = 3.213, P = .523	H (4, N = 122) = 12.341, P = .015
	si1 (ND)	pA (0.200 ± 0.115) a	sA (ND)
	si2 (0.167 ± 0.167) a	pB (0.417 ± 0.376) a	sB (ND)
	si3 (0.250 ± 0.211) a	pC (0.667 ± 0.457) a	sC (0.250 ± 0.183) a
	si4 (0.083 ± 0.083) a	pD (ND)	sD (0.458 ± 0.417) a
	si5 (0.960 ± 0.524) a	pE (0.200 ± 0.163) a	sE (0.760 ± 0.405) a
Acer barbinerve	H (4, N = 122) = 20.218, P < .001	H (4, N = 122) = 7.523, P = .111	H (4, N = 122) = 32.937, P < .001
	si1 (2.080 ± 0.562) b	pA (3.600 ± 0.808) a	sA (2.600 ± 0.638) b
	si2 (5.208 ± 0.866) a	pB (5.375 ± 0.884) a	sB (2.458 ± 0.542) b
	si3 (6.292 ± 1.214) a	pC (4.750 ± 1.043) a	sC (6.542 ± 1.075) a
	si4 (5.875 ± 1.010) a	pD (5.958 ± 1.136) a	sD (6.708 ± 1.225) a
	si5 (7.600 ± 1.190) a	pE (7.320 ± 1.241) a	sE (8.680 ± 1.027) a
Acer pseudo-siebodianum	H (4, N = 122) = 18.599, P < .001	H (4, N = 122) = 13.988, P = .007	H (4, N = 122) = 30.115, P < .001
	si1 (3.760 ± 1.040) b	pA (3.840 ± 0.916) b	sA (2.360 ± 0.693) b
	si2 (7.542 ± 1.280) a	pB (8.667 ± 1.328) a	sB (7.125 ± 1.050) a
	si3 (7.958 ± 1.067) a	pC (7.708 ± 1.448) ab	sC (8.500 ± 1.424) a
	si4 (7.333 ± 1.196) a	pD (8.458 ± 1.025) a	sD (8.917 ± 1.225) a
	si5 (9.640 ± 1.163) a	pE (7.640 ± 1.039) a	sE (9.400 ± 0.985) a

Such a "high-west vs. low-east" moisture/nutrient gradient was confirmed by the current study, i.e., the western areas had higher soil nutrient levels and WC than those of the eastern areas and positive correlations were observed between WC and soil nutrient contents (Fig. 1, Fig. S2). This finding is supported by the fact that a moisture gradient accompanies forest floor organic matter (e.g., organic C, total N and P) accumulation because of the discharge of water from higher to lower sites (Meier and Leuschner, 2014; Toljander et al., 2006).

4.1.2. Site and vegetation interaction

A natural spatial floristic transect revealed that pioneer species (e.g., *Betula platyphylla*) occurred at si1, whereas late-stage species (e.g., *Tilia mandshurica* and *Ulmus laciniata*) occurred at si5 (Table 1). Furthermore, *Betula platyphylla* vs. *Ulmus laciniata* occurred in the opposite direction along CCA1 (Fig. 1). Moreover, y vs. x showed opposite relationships with *Betula platyphylla* vs. *Ulmus laciniata* (Fig. 1).

Table 2
ECM fungal alpha-diversity as affected by environmental gradients
Using "quantile" and grade score divisions at 0.8, 0.6, 0.4, and 0.2, we obtain five gradients of geographical site according to site_score: si1, scores > 0.8; si2, scores between 0.6 and 0.8; si3, scores between 0.4 and 0.6; si4, scores between 0.2 and 0.4; si5, scores < 0.2. Thus, plots from site1 to site5 separately distribute from northwest to southeast. Similarly, we establish five gradients of soil nutrient (soil_Gr), comprising sA, sB, sC, sD and sE, and five gradients of plant function index (plant_Gr), comprising pA, pB, pC, pD and pE. The abundances of key tree species (mean ± SE) at different environmental gradient levels are given in parentheses. Different letters between environmental gradients indicate significant differences at the P < .05 significance level as determined by nonparametric analyses (Kruskal-Wallis test) in Statistica 10 (StatSoft Inc., Tulsa, Okla., USA).

ECM diversity	Gr_site	Gr_plant	Gr_soil
Abundance%	H (4, N = 114) = 7.064, P = .133	H (4, N = 122) = 11.264, P = .024	H (4, N = 120) = 15.603, P = .004
	si1 (41.996 ± 4.313) a	pA (36.475 ± 5.039) ab	sA (33.847 ± 4.170) b
	si2 (49.411 ± 5.454) a	pB (52.350 ± 5.002) a	sB (46.385 ± 5.369) ab
	si3 (48.205 ± 4.086) a	pC (33.063 ± 4.213) b	sC (47.555 ± 4.762) ab
	si4 (41.553 ± 3.445) a	pD (43.961 ± 4.646) ab	sD (32.902 ± 4.000) b
	si5 (33.639 ± 4.892) a	pE (49.177 ± 4.132) ab	sE (54.240 ± 4.090) a
S.cum	H (4, N = 119) = 13.472, P = .009	H (4, N = 119) = 5.319, P = .256	H (4, N = 119) = 9.229, P = .056
	si1 (129.583 ± 4.159) b	pA (128.625 ± 5.210) a	sA (126.040 ± 4.846) b
	si2 (127.250 ± 4.415) b	pB (133.727 ± 4.008) a	sB (134.091 ± 3.596) ab
	si3 (148.708 ± 4.290) a	pC (135.167 ± 5.853) a	sC (136.652 ± 4.786) ab
	si4 (136.217 ± 5.440) ab	pD (138.750 ± 3.783) a	sD (141.917 ± 4.852) ab
	si5 (143.583 ± 4.655) ab	pE (143.800 ± 4.916) a	sE (146.280 ± 5.064) a
Shannon	H (4, N = 119) = 4.825, P = .306	H (4, N = 115) = 1.686, P = .793	H (4, N = 119) = 3.676, P = .452
	si1 (2.653 ± 0.118) a	pA (2.589 ± 0.108) a	sA (2.576 ± 0.100) a
	si2 (2.359 ± 0.125) a	pB (2.475 ± 0.089) a	sB (2.539 ± 0.122) a
	si3 (2.526 ± 0.101) a	pC (2.558 ± 0.118) a	sC (2.320 ± 0.113) a
	si4 (2.419 ± 0.085) a	pD (2.460 ± 0.104) a	sD (2.601 ± 0.094) a
	si5 (2.639 ± 0.095) a	pE (2.458 ± 0.110) a	sE (2.559 ± 0.100) a
Simpson	H (4, N = 114) = 10.080, P = .039	H (4, N = 115) = 2.356, P = .671	H (4, N = 113) = 6.234, P = .182
	si1 (0.874 ± 0.010) a	pA (0.849 ± 0.014) a	sA (0.853 ± 0.011) a
	si2 (0.777 ± 0.030) b	pB (0.829 ± 0.017) a	sB (0.824 ± 0.022) a
	si3 (0.847 ± 0.013) ab	pC (0.860 ± 0.012) a	sC (0.802 ± 0.020) a
	si4 (0.818 ± 0.014) b	pD (0.823 ± 0.018) a	sD (0.870 ± 0.010) a
	si5 (0.859 ± 0.014) ab	pE (0.833 ± 0.020) a	sE (0.847 ± 0.014) a
Inver_Simpson	H (4, N = 109) = 5.145, P = .273	H (4, N = 115) = 1.591, P = .811	H (4, N = 109) = 10.104, P = .039
	si1 (6.917 ± 0.657) a	pA (6.731 ± 0.573) a	sA (6.441 ± 0.546) ab
	si2 (6.683 ± 0.824) a	pB (6.739 ± 0.740) a	sB (6.690 ± 0.770) ab
	si3 (5.934 ± 0.473) a	pC (6.808 ± 0.662) a	sC (4.669 ± 0.397) b
	si4 (5.313 ± 0.348) a	pD (5.738 ± 0.507) a	sD (7.503 ± 0.638) a
	si5 (7.170 ± 0.646) a	pE (6.859 ± 0.745) a	sE (6.591 ± 0.627) ab
J_Evenness	H (4, N = 116) = 2.997, P = .558	H (4, N = 115) = 1.628, P = .804	H (4, N = 119) = 4.645, P = .326
	si1 (0.523 ± 0.019) a	pA (0.521 ± 0.020) a	sA (0.530 ± 0.016) a
	si2 (0.488 ± 0.026) a	pB (0.502 ± 0.017) a	sB (0.505 ± 0.021) a
	si3 (0.505 ± 0.019) a	pC (0.510 ± 0.020) a	sC (0.470 ± 0.022) a
	si4 (0.498 ± 0.013) a	pD (0.499 ± 0.021) a	sD (0.527 ± 0.019) a
	si5 (0.532 ± 0.019) a	pE (0.495 ± 0.021) a	sE (0.515 ± 0.018) a

Similar spatial differentiation was identified in our previous reports: 1) the nutrient-rich habitat (low plateau to the west) is characteristic of higher forest recruitment rates (stems < 1 cm) (Yuan et al., 2016), and 2) soil moisture and topographic conditions influence the spatial distribution of plants, with the stems of *Q. mongolica* (shade-intolerant species) in upper height classes being mostly distributed in the east and those of the sapling and lower height classes being most prevalent in the northwest (Hao et al., 2007).

This local-scale forest transect might have begun with an accidental disturbance decades ago. For instance, several late-stage trees might have been destroyed due to the highly frequent strong winds in the early spring and winter (Yuan et al., 2016). Another likely fatal disturbance is disease, which occurs occasionally, as nutrient (e.g., N) enrichment in the western areas might predispose the vegetation to increased incidence and severity of disease infection (Lopez-Zamora et al., 2007). Subsequently, *Betula platyphylla*, a very common and important species at the initial stage of forest establishment (Nara, 2006b) due to its wind-spread/winged nuts and light-promoted sapling growth (Dolezal et al., 2004; Haruki and Tsuyuzaki, 2001; Jia et al., 2016), might have been introduced to this disturbed area.

4.1.3. Vegetation and soil interaction

Strong environmental filtering effects on vegetation life strategies and functional traits have been consistently identified across high- to low-nutrient stress gradients (Hao et al., 2007; Higgins et al., 2014; Ruotsalainen et al., 2009). We observed contrasting distributions of *Betula platyphylla* vs. *Tilia mandshurica* along the soil nutrient gradients (Table 1). Specifically, soil nutrients (e.g., SOM) and pioneer trees (*Betula platyphylla* and *Syringa reticulata*) were positively related to LNC and SRL (Fig. 1). These relationships occurred because compared with late-stage vegetation species, fast-growing pioneer vegetation species (e.g., *Betula platyphylla*) invest more in light acquisition and photosynthetic product allocation (e.g., by increasing LNC) (Higgins et al., 2014; Sawada et al., 2015), and they develop advanced fine roots as an adaptation to promote nutrient absorption (e.g., by increasing SRL) (Meier and Leuschner, 2014).

In contrast, late-stage vegetation species (*Ulmus laciniata* and *Tilia mandshurica*) were highly favored in low-moisture and nutrient-poor environments and positively correlated with plant functional diversity (e.g., FD.lpc) but negatively related to SRL, LNC and LA (Fig. 1). These findings suggest that nutrient-poor environments result in less dependence on light acquisition and soil-borne nutrient sources by increasing nutrient-cycling efficiency (e.g., P allocation and resorption) (Higgins et al., 2014; Meier and Leuschner, 2014). Moreover, shade-tolerant species can persist on resource-poor soils because their small and thick leaves can decrease transpiration and/or nutrient loss and allow the plant to adapt to water stress and nutrient shortages (Sawada et al., 2015; Turner et al., 2018).

Table 3
The abundances of 15 Key ECM fungal groups as affected by environmental gradients.
Using "quantile" and grade score divisions at 0.8, 0.6, 0.4, and 0.2, we obtain five gradients of geographical site according to site_score: si1, scores > 0.8; si2, scores between 0.6 and 0.8; si3, scores between 0.4 and 0.6; si4, scores between 0.2 and 0.4; si5, scores < 0.2. Thus, plots from site1 to site5 separately distribute from northwest to southeast. Similarly, we establish five gradients of soil nutrient (soil_Gr), comprising sA, sB, sC, sD and sE, and five gradients of plant function index (plant_Gr), comprising pA, pB, pC, pD and pE. The abundances of key tree species (mean ± SE) at different environmental gradient levels are given in parentheses. Different letters between environmental gradients indicate significant differences at the $P < .05$ significance level as determined by nonparametric analyses (Kruskal-Wallis test) in Statistica 10 (StatSoft Inc., Tulsa, Okla., USA).

ECM groups	Gr_site	Gr_plant	Gr_soil
KeyG1	H (4, N = 122) = 4.767, P = .312	H (4, N = 122) = 1.632, P = .803	H (4, N = 122) = 1.530, P = .821
	si1 (0.065 ± 0.047) a	pA (0.116 ± 0.063) a	sA (0.155 ± 0.100) a
	si2 (0.581 ± 0.382) a	pB (0.480 ± 0.380) a	sB (0.063 ± 0.049) a
	si3 (0.067 ± 0.054) a	pC (0.105 ± 0.060) a	sC (0.411 ± 0.375) a
	si4 (0.035 ± 0.014) a	pD (0.029 ± 0.014) a	sD (0.059 ± 0.028) a
	si5 (0.372 ± 0.357) a	pE (0.387 ± 0.361) a	sE (0.425 ± 0.359) a
KeyG2	H (4, N = 122) = 13.715, P = .008	H (4, N = 122) = 5.484, P = .241	H (4, N = 122) = 10.428, P = .034
	si1 (0.002 ± 0.001) b	pA (0.011 ± 0.009) a	sA (0.002 ± 0.001) b
	si2 (0.011 ± 0.009) ab	pB (0.799 ± 0.744) a	sB (0.005 ± 0.002) ab
	si3 (0.616 ± 0.557) ab	pC (0.572 ± 0.558) a	sC (0.017 ± 0.010) ab
	si4 (0.003 ± 0.001) ab	pD (0.291 ± 0.285) a	sD (0.293 ± 0.285) ab
	si5 (1.005 ± 0.755) a	pE (0.005 ± 0.002) a	sE (1.308 ± 0.873) a
KeyG3	H (4, N = 122) = 9.644, P = .047	H (4, N = 122) = 3.782, P = .436	H (4, N = 122) = 5.399, P = .249
	si1 (0.400 ± 0.385) a	pA (0.387 ± 0.386) a	sA (0.007 ± 0.005) a
	si2 (0.001 ± 0.001) ab	pB (0.009 ± 0.006) a	sB (0.010 ± 0.007) a
	si3 (0.010 ± 0.006) ab	pC (0.011 ± 0.007) a	sC (0.402 ± 0.402) a
	si4 (0.002 ± 0.001) ab	pD (0.004 ± 0.003) a	sD (0.002 ± 0.001) a
	si5 (0.001 ± 0.001) b	pE (0.001 ± 0.001) a	sE (0.007 ± 0.006) a
KeyG4	H (4, N = 122) = 6.759, P = .149	H (4, N = 122) = 0.803, P = .938	H (4, N = 122) = 1.853, P = .763
	si1 (3.866 ± 2.242) a	pA (0.753 ± 0.689) a	sA (2.277 ± 1.586) a
	si2 (0.381 ± 0.199) a	pB (2.578 ± 1.655) a	sB (2.339 ± 1.747) a
	si3 (0.122 ± 0.078) a	pC (0.437 ± 0.278) a	sC (0.062 ± 0.016) a
	si4 (1.570 ± 0.857) a	pD (0.268 ± 0.167) a	sD (0.949 ± 0.713) a
	si5 (0.429 ± 0.264) a	pE (2.380 ± 1.709) a	sE (0.791 ± 0.510) a
KeyG5	H (4, N = 122) = 11.140, P = .025	H (4, N = 122) = 0.429, P = .980	H (4, N = 122) = 2.345, P = .673
	si1 (0.003 ± 0.003) b	pA (0.179 ± 0.158) a	sA (0.005 ± 0.003) a
	si2 (0.182 ± 0.165) ab	pB (0.010 ± 0.005) a	sB (0.115 ± 0.093) a
	si3 (0.017 ± 0.011) ab	pC (0.111 ± 0.093) a	sC (0.187 ± 0.165) a
	si4 (0.094 ± 0.093) ab	pD (0.013 ± 0.011) a	sD (0.002 ± 0.001) a
	si5 (0.028 ± 0.012) a	pE (0.004 ± 0.003) a	sE (0.015 ± 0.006) a
KeyG6	H (4, N = 122) = 11.387, P = .023	H (4, N = 122) = 6.619, P = .157	H (4, N = 122) = 5.118, P = .275
	si1 (0.193 ± 0.104) ab	pA (0.539 ± 0.341) a	sA (0.197 ± 0.104) a
	si2 (0.071 ± 0.031) a	pB (0.012 ± 0.003) a	sB (0.041 ± 0.026) a
	si3 (0.029 ± 0.016) ab	pC (0.036 ± 0.015) a	sC (0.038 ± 0.019) a
	si4 (0.008 ± 0.003) b	pD (0.549 ± 0.504) a	sD (0.509 ± 0.505) a
	si5 (0.842 ± 0.576) ab	pE (0.027 ± 0.018) a	sE (0.377 ± 0.332) a
KeyG7	H (4, N = 122) = 1.847, P = .764	H (4, N = 122) = 3.925, P = .416	H (4, N = 122) = 7.248, P = .123
	si1 (0.002 ± 0.002) a	pA (0.098 ± 0.087) a	sA (0.001 ± 0.001) a
	si2 (0.012 ± 0.010) a	pB (0.012 ± 0.010) a	sB (0.003 ± 0.002) a
	si3 (0.048 ± 0.036) a	pC (0.037 ± 0.035) a	sC (0.011 ± 0.011) a
	si4 (0.005 ± 0.004) a	pD (0.003 ± 0.002) a	sD (0.003 ± 0.001) a
	si5 (0.089 ± 0.087) a	pE (0.005 ± 0.004) a	sE (0.136 ± 0.092) a
KeyG8	H (4, N = 122) = 9.904, P = .042	H (4, N = 122) = 9.054, P = .060	H (4, N = 122) = 6.240, P = .182
	si1 (0.006 ± 0.002) a	pA (0.057 ± 0.048) a	sA (0.005 ± 0.002) a
	si2 (0.004 ± 0.004) b	pB (0.003 ± 0.001) ab	sB (0.129 ± 0.088) a
	si3 (0.077 ± 0.075) ab	pC (0.004 ± 0.002) ab	sC (0.006 ± 0.004) a
	si4 (0.056 ± 0.050) ab	pD (0.077 ± 0.075) ab	sD (0.007 ± 0.004) a
	si5 (0.005 ± 0.001) a	pE (0.005 ± 0.004) b	sE (0.002 ± 0.001) a
KeyG9	H (4, N = 122) = 31.795, P < .001	H (4, N = 122) = 8.551, P = .073	H (4, N = 122) = 9.157, P = .057
	si1 (0.019 ± 0.013) b	pA (1.557 ± 1.540) a	sA (0.035 ± 0.016) b
	si2 (0.007 ± 0.003) b	pB (0.120 ± 0.055) b	sB (0.246 ± 0.207) ab
	si3 (1.901 ± 1.604) a	pC (0.287 ± 0.215) ab	sC (1.689 ± 1.602) ab
	si4 (0.209 ± 0.085) a	pD (0.069 ± 0.027) ab	sD (0.337 ± 0.202) a
	si5 (0.717 ± 0.474) a	pE (0.755 ± 0.469) ab	sE (0.553 ± 0.440) ab
KeyG10	H (4, N = 122) = 4.350, P = .361	H (4, N = 122) = 4.484, P = .344	H (4, N = 122) = 3.747, P = .441
	si1 (0.447 ± 0.361) a	pA (2.010 ± 1.656) a	sA (0.034 ± 0.020) a
	si2 (2.106 ± 1.718) a	pB (0.393 ± 0.372) a	sB (0.849 ± 0.445) a
	si3 (0.873 ± 0.426) a	pC (0.004 ± 0.002) a	sC (2.070 ± 1.725) a
	si4 (0.208 ± 0.098) a	pD (0.717 ± 0.319) a	sD (0.238 ± 0.166) a
	si5 (0.262 ± 0.247) a	pE (0.689 ± 0.354) a	sE (0.705 ± 0.366) a
KeyG11	H (4, N = 122) = 11.521, P = .021	H (4, N = 122) = 5.747, P = .219	H (4, N = 122) = 5.313, P = .257
	si1 (0.017 ± 0.006) ab	pA (0.062 ± 0.042) a	sA (0.027 ± 0.013) a
	si2 (1.937 ± 1.920) b	pB (0.086 ± 0.057) a	sB (0.156 ± 0.146) a
	si3 (1.609 ± 1.174) ab	pC (0.035 ± 0.023) a	sC (1.992 ± 1.918) a
	si4 (0.423 ± 0.351) ab	pD (0.454 ± 0.401) a	sD (2.765 ± 1.465) a
	si5 (2.272 ± 1.358) a	pE (5.485 ± 2.383) a	sE (1.356 ± 1.084) a
KeyG12	H (4, N = 122) = 3.225, P = .521	H (4, N = 122) = 5.426, P = .246	H (4, N = 122) = 1.100, P = .894
	si1 (0.393 ± 0.182) a	pA (0.277 ± 0.120) a	sA (0.131 ± 0.070) a
	si2 (2.476 ± 2.384) a	pB (2.153 ± 1.808) a	sB (0.108 ± 0.075) a

(continued on next page)

Table 3 (*continued*)

ECM groups	Gr_site	Gr_plant	Gr_soil
	si3 (0.133 ± 0.083) a	pC (0.055 ± 0.026) a	sC (2.499 ± 2.384) a
	si4 (1.961 ± 1.809) a	pD (0.066 ± 0.032) a	sD (1.879 ± 1.811) a
	si5 (0.049 ± 0.026) a	pE (2.369 ± 2.289) a	sE (0.392 ± 0.177) a
KeyG13	H (4, N = 122) = 13.140, P = .011	H (4, N = 122) = 6.997, P = .136	H (4, N = 122) = 17.213, P = .002
	si1 (0.001 ± 0.001) b	pA (0.001 ± 0.001) a	sA (0.001 ± 0.001) b
	si2 (0.005 ± 0.003) ab	pB (0.001 ± 0.001) a	sB (0.001 ± 0.001) b
	si3 (0.365 ± 0.364) ab	pC (0.006 ± 0.003) a	sC (0.004 ± 0.003) ab
	si4 (0.001 ± 0.001) ab	pD (0.366 ± 0.364) a	sD (0.003 ± 0.001) a
	si5 (0.002 ± 0.001) a	pE (0.001 ± 0.001) a	sE (0.351 ± 0.349) ab
KeyG14	H (4, N = 122) = 4.446, P = .349	H (4, N = 122) = 1.843, P = .765	H (4, N = 122) = 4.622, P = .328
	si1 (0.068 ± 0.067) a	pA (0.010 ± 0.009) a	sA (0.002 ± 0.001) a
	si2 (0.027 ± 0.021) a	pB (1.891 ± 1.497) a	sB (0.256 ± 0.195) a
	si3 (0.201 ± 0.184) a	pC (0.004 ± 0.002) a	sC (0.008 ± 0.005) a
	si4 (0.011 ± 0.007) a	pD (0.213 ± 0.185) a	sD (0.460 ± 0.424) a
	si5 (1.844 ± 1.437) a	pE (0.107 ± 0.071) a	sE (1.446 ± 1.395) a
KeyG15	H (4, N = 122) = 15.281, P = .004	H (4, N = 122) = 4.008, P = .405	H (4, N = 122) = 9.363, P = .053
	si1 (0.023 ± 0.021) ab	pA (0.052 ± 0.033) a	sA (0.053 ± 0.035) ab
	si2 (0.032 ± 0.031) b	pB (1.849 ± 1.357) a	sB (0.175 ± 0.167) b
	si3 (0.063 ± 0.030) a	pC (0.685 ± 0.512) a	sC (0.544 ± 0.492) ab
	si4 (1.379 ± 0.966) ab	pD (0.049 ± 0.034) a	sD (0.539 ± 0.492) ab
	si5 (2.392 ± 1.361) a	pE (1.298 ± 0.929) a	sE (2.568 ± 1.502) a

4.2. ECM fungal communities differentiate along environmental gradients

4.2.1. General description

In this study, 122 grids were investigated, and at least 28,881 reads per sample were obtained, contributing to the identification of over 1000 assigned ECM fungal species. Previously, a total of 2706 OTUs and 54 lineages of ECM fungi were identified in 760 soil samples across 30 Fagaceae forest sites in China (Wu et al., 2018). As previously reported (Coince et al., 2013), soil can be a good substitute for fine roots in studying ECM fungi. Moreover, the 65 primary ECM fungal species in the current study are affiliated with common ECM fungal genera (e.g., *Tomentella*, *Cortinarius*, *Russula*, *Inocybe* and *Russulaceae*) and have frequently been encountered (Bahram et al., 2013; Põlme et al., 2013; Richard et al., 2005).

4.2.2. Soil and site effects

ECM fungal communities were more abundant in nutrient-poor and low-moisture environments (i.e., sA < sE; Table 2), and most of the key ECM fungal species were negatively related to soil nutrients (Fig. 3). In addition, the relative abundances of some ECM fungal groups (e.g., KeyG2 and KeyG15) significantly increased in southeastern (si5) areas and were correlated with the geographical coordinate (x) (Table 3, Fig. 3). Previous studies have also reported that ECM fungal communities are 1) negatively related to the soil nutrient status (e.g., SOM, P and N) (Kumar and Atri, 2017), 2) more abundant in nutrient-poor sites (Ruotsalainen et al., 2009), and 3) separated into lower (plots at 200–600 m) and higher (plots at 800–1200 m) elevation classes (Matsuoka et al., 2016). Such dominant ECM symbioses under nutrient-deficiecy lie in immediate contact with surrounding soil nutrients (Kumar and Atri, 2017; Ruotsalainen et al., 2009) and increased production of ECM roots in response to plant nutrient acquisition (Hagerberg et al., 2003).

Particularly, the relative abundances of KeyG2 (including *Russula*, *Amanita* and *Sebacina*) and KeyG15 (including *Timgrovea* and *Tricholoma*) increased not only along the sA-sE gradient but also along the si1-si5 gradient (Table 3), and they were more abundant in the eastern areas than in the western areas (i.e., positively related to x) and negatively influenced by chemical properties (especially for WC, SOM and AN) (Fig. 3). These results can be expected because the genera *Russula* and *Amanita* and *Timgrovea* are often adapted to drought (Azul et al., 2010; Lilleskov et al., 2009; Vernes et al., 2001) and the genus *Sebacina* significantly promotes plant root growth by increasing nutrient sequestration and anchoring soil under severe drought conditions (Ghimire and Craven, 2011). Moreover, the genus *Tricholoma* was reported to be negatively related to the availability of soil nutrients (Lilleskov et al., 2002; Lilleskov et al., 2011) and thus preferred nutrient-deficient sites to the east (Fig. 3).

In contrast, high soil moisture and SOM content caused by leaching from high (eastern) to low (western) areas in the current study might have promoted aboveground biomass and substrate immobilization in the soil by increasing the decomposition of litterfall (Haruki and Tsuyuzaki, 2001; Meier and Leuschner, 2014; Takyu et al., 2002; Yuan et al., 2016). Thus, the reduction in ECM growth under a high nutrient status (e.g., sA and si1) might have been caused by indirect inhibition of host tree growth (Cairney, 2012) or by increased foliar litter input driven by competition of saprotrophic growth (especially input from those species with higher LNC) (Otsing et al., 2018) and soil resource abundance (e.g., SOM and WC) (Talbot et al., 2013).

In addition, of the 65 key species in the current study, we found five ascomycetes, including one *Hydnobolites* (not affiliated to any key ECM group), one *Genea* in KeyG1, and two *Elaphomyces* and one *Hydnobolites* in KeyG8 (Fig. 3). Generally, ECM ascomycetes do not perform sexual reproduction but may produce lignolytic enzymes as well as conidia and chlamydospores (Tedersoo et al., 2010). ECM ascomycetes are supposed to be stress-tolerant species and highly resistant to drought (Ruotsalainen et al., 2009). However, we found that only G8_*Elaphomyces muricatu* was significantly and negatively related to WC (P < .05; Fig. 3).

4.2.3. Soil and vegetation effects

Ulmus laciniata and *Tilia mandshurica* showed significant and positive relationships with genera from KeyG2 (*Amanita*, *Hydnum*, *Russula*, *Sebacina* and *Tomentella*), KeyG5 (e.g., *Inocybe*), KeyG14 (*Tylospora* and *Russula*) and KeyG15 (*Cortinarius*, *Timgrovea* and *Tricholoma*) (Fig. 3); all these tree species and ECM genera were significantly and negatively correlated with soil nutrients, such as WC, SOM and AN (Fig. 1, Fig. 3). Similarly, ECM fungi in infertile environments have been reported to be dominated by *Tomentella*, *Cortinarius* and *Sebacina* (Ryberg et al., 2009). Furthermore, *Cortinarius*, *Sebacina*, *Russula* and *Inocybe* fungi are closely related to late-stage host growth (Hewitt et al., 2017; Long et al., 2016; Nara et al., 2003; Obase et al., 2009), and primarily endomycorrhizal *Tilia* trees are regularly associated with the genera *Russula* and *Inocybe* (Cui and Mu, 2016; Krivtsov et al., 2003).

Late-stage vegetation that persists for decades allows for the continuous selection of fungal recruitment and thus hosts aging-related accumulation in specific ECM fungal communities in mature forests (Taudiere et al., 2015). Moreover, the late-stage vegetation associated

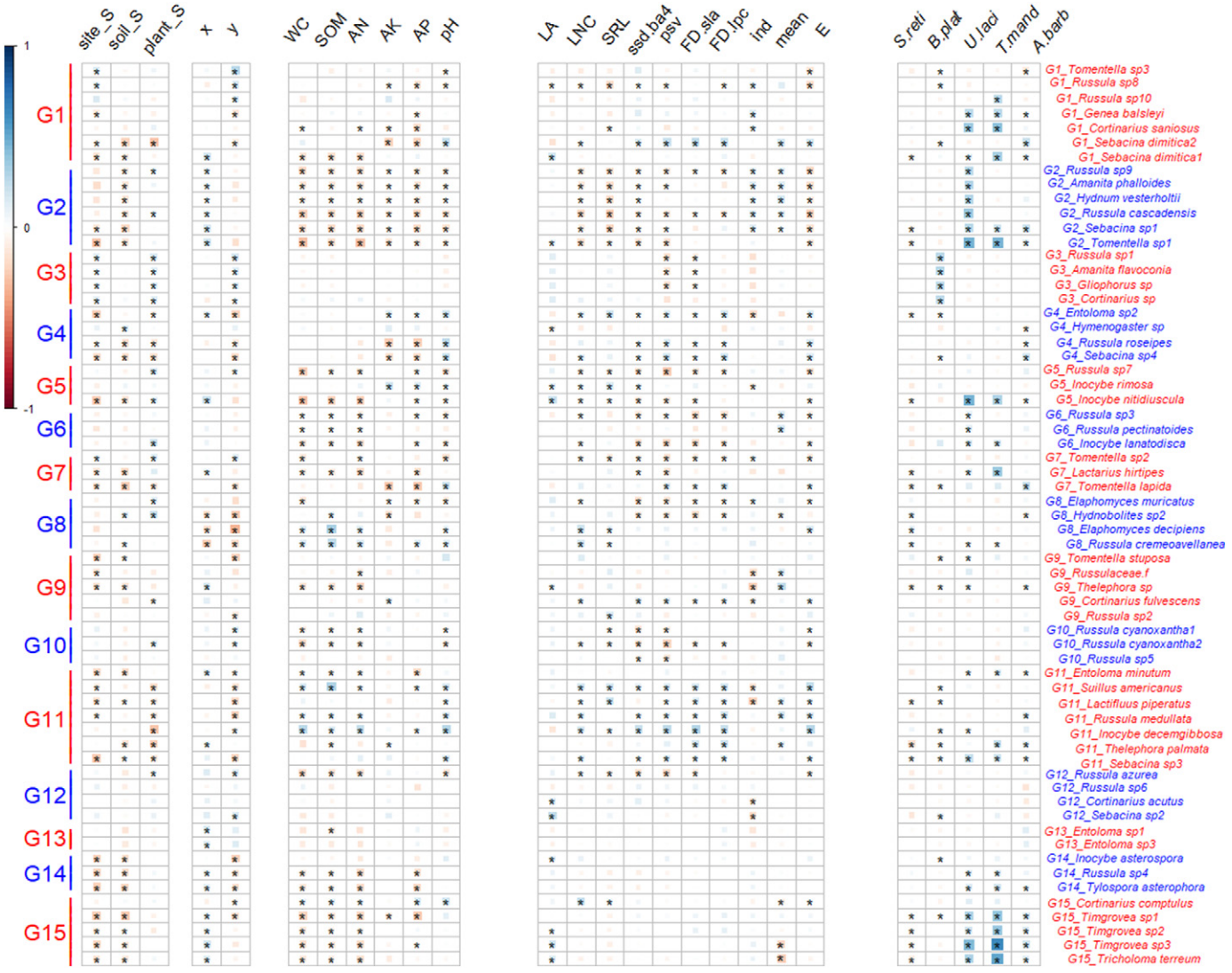

Fig. 3. Correlation analyses between the environmental variables and 15 groups of ECM fungal species. Correlation analysis is conducted with the corrplot package in R. Pearson r linear correlation is computed on standardized variables. The composite scores include geographic parameters (site_S), soil chemical properties (soil_S) and vegetation function traits (plant_S). The geographical variables include longitude (x) and latitude (y). Soil chemical properties include water content (WC), soil organic matter (SOM), available N (AN), available K (AK), available P (AP) and pH. Vegetation functional traits include leaf area (LA), leaf nitrogen content (LNC), specific root length (SRL), community structure diversity indexes based on average diameter at breast height of 4 cm (ssd.ba4), phylogenetic species variability (psv), specific leaf area (FD.sla), leaf phosphorus content (FD.lpc), stem density (ind), the average aboveground biomass of three forest inventories (mean) and evenness (E). Key tree species are denoted by *S. reti* (*Syringa reticulata*), *B. plat* (*Betula platyphylla*), *U. laci* (*Ulmus laciniata*), *T. mand* (*Tilia mandshurica*) and *A. barb* (*Acer barbinerve*). *, P < .05.

genera are reported to produce copious hyphal strands emanating from the sheath surface, which may help to exclude competitors (Pickles et al., 2010). All these factors can explain why the late-stage KeyG2 species were positively related to the average vegetation biomass (mean) and stem density (ind) but negatively related to floristic diversity (E) (Fig. 3).

In contrast, members of KeyG8 (e.g., *Elaphomyces* and *Russula*) and KeyG11 (e.g., *Suillus, Inocybe* and *Russula*) were positively related to LNC, SRL and SOM (Fig. 3). Moreover, the relative abundances of KeyG8 members declined along plant_Gr (Table 3). The genus *Russula* network is believed to have a positive effect on mobilizing labile N sources and thus results in lower foliar C/N in seedlings (such as aspen, spruce, birch) (Hewitt et al., 2017; Nara, 2006a). Furthermore, seedlings colonized by *Elaphomyces* exhibit more efficient mobilization of organic N from complex organic polymers (Turnbull et al., 1995). Moreover, the genus *Elaphomyces* is closely related to root length (Gandini et al., 2015). Thus, the ECM symbiont can implement vegetation life strategies by increasing fine-root nutrient acquisition efficiency under a high nutrient status (Ostonen et al., 2011).

4.2.4. Vegetation and site effects

The middle gradient sites (si2 or si3) had the highest values of ECM fungal abundance and S.cum (Table 2). First, the middle gradient sites (si2 or si3) were either encountered with early-stage (*Ulmus japonica, Syringa reticulata* and *Maackia amurensis*) or late-stage (*Ulmus laciniata* and *Tilia mandshurica*) vegetation (Table 1). Second, ECM species composition and colonization can be significantly influenced by vegetation composition, especially in terms of host identity (Hewitt et al., 2017; Jonsson et al., 1999; Lofgren et al., 2018), and different life-strategy vegetation (such as early-successional vs. late-successional trees) may have different associated ECM fungal species (Taudiere et al., 2015). Therefore, as previously reported (Asplund et al., 2019; Toljander et al., 2006), mixed-forest stands (i.e., si2 and si3) encountered the highest number of ECM taxa.

Such a "middle gradient effect" (or "mixed-forest effect") was also observed with KeyG9 (Table 3). This result occurred because the KeyG9 includes *Russula* and *Cortinarius* (Fig. 3), which are closely associated with either early-stage (Clemmensen et al., 2015; Hewitt et al., 2017; Nara, 2006a; van der Heijden and Kuyper, 2003) or late-stage

characteristics (Cui and Mu, 2016; Krivtsov et al., 2003; Pickles et al., 2010). Together, the highest frequencies and abundances of ECM symbioses at the middle sites si2–si3 confirm a floristic gradient transect existing along this 25-hm^2 plot (Table 2).

4.3. Conclusions and implications: ECM-associated determinants jointly reflect ecological processes

In this study, a total of 25 environmental variables closely associated with ECM fungal composition were separately combined into three categories of composite scores and then applied to quantify environmental quality gradients of geographical sites, soil chemical properties and vegetation functional traits. Similarly, the environmental quality has been evaluated in previous studies, such as soil quality based upon edaphic properties (Nabiollahi et al., 2018; Tuomisto et al., 2002), floristic gradients derived from plant species composition (Riedler and Lang, 2018; Tuomisto et al., 2018), and spatially explicit patterns along geographic coordinates (Normand et al., 2009; Wasof et al., 2013). By considering the influences and interactions of the above environmental quality gradients, the shifts in floristic composition and ECM fungal community structure and diversity were successfully presented and explained in the context of biotic adaptations and abiotic variances in this study. The biotic adaptations were determined by vegetation functional traits and ECM fungal abundance and diversity, whereas the environmental variances reflected the spatial heterogeneity determined by topographic differences and soil chemical properties.

Specifically, the occurrence of early-stage *Betula platyphylla* and *Syringa reticulata* and the lack of late-stage *Ulmus laciniata* and *Tilia mandshurica* vegetation in the northwestern areas (e.g., si1) suggest that forest succession should have been interrupted and that disturbance might have occurred in the past. However, the lack of *Betula platyphylla* in the southeastern areas (e.g., si5) indicates that the long-term forest succession processes had rarely been interrupted. The site_score and soil_score similarly showed negative relationships with ECM diversity (e.g., S.cum) as well as with the relative abundances (%) of KeyG2, 11, 14 and 15 (Fig. 2, Fig. 3). Specifically, the KeyG15 significantly increased along site_Gr (from si1 to si5) as well as soil_Gr (from sA to sE) (Table 3). All these findings confirm that most ECM fungal groups can influence floristic functional traits by highly efficient nutrient mining and nonstructural carbohydrate redistribution in tree organs under nutrient stress and drought environments.

The abovementioned environmental gradient effects and the positive correlations among the three types of ECM-associated composite scores strongly confirm our hypotheses that the ECM fungal community is a pivotal interface/proxy for the investigation of historical and potential environmental processes that shape site-specific soil properties and vegetation composition. Furthermore, strong within-site correlations between ECM composition, tree species and soil properties are closely related to geographical parameters or the impacts of natural spatial heterogeneity at a local scale. These data demonstrate the importance of ECM fungal habitat isolation and dispersal limitation in determining host-range expansion. Thus, predictions of ecological process and forest stand development should be carried out in the context of ECM-associated variables.

Acknowledgments

This work was supported by the National Natural Science Foundation of China (31722010, 31670506, 41671050) and the National Key Research and Development Program of China (2016YFC0500300).

Author contributions

Z.B. X.W. and H.Y. conceived the idea of this study. Z.Y., D.W., S.F. and J.Y. collected the data. Z.B. wrote the first draft of the manuscript and all the authors contributed substantially to the revisions.

Declaration of competing interest

The authors declare that they have no conflict of interest.

Appendix A. Supplementary data

Supplementary data to this article can be found online at https://doi.org/10.1016/j.scitotenv.2019.135475.

References

Ali, A., Yan, E.-R., Chen, H.Y.H., Chang, S.X., Zhao, Y.-T., Yang, X.-D., et al., 2016. Stand structural diversity rather than species diversity enhances aboveground carbon storage in secondary subtropical forests in Eastern China. Biogeosciences 13, 4627–4635.
Ali, A., Yan, E.R., Chang, S.X., Cheng, J.Y., Liu, X.Y., 2017. Community-weighted mean of leaf traits and divergence of wood traits predict aboveground biomass in secondary subtropical forests. Sci. Total Environ. 574, 654–662.
Aponte, C., García, L.V., Marañón, T., Gardes, M., 2010. Indirect host effect on ectomycorrhizal fungi: leaf fall and litter quality explain changes in fungal communities on the roots of co-occurring Mediterranean oaks. Soil Biol. Biochem. 42, 788–796.
Asplund, J., Kauserud, H., Ohlson, M., Nybakken, L., 2019. Spruce and beech as local determinants of forest fungal community structure in litter, humus and mineral soil. FEMS Microbiol. Ecol. 95.
Azul, A.M., Sousa, J.P., Agerer, R., Martin, M.P., Freitas, H., 2010. Land use practices and ectomycorrhizal fungal communities from oak woodlands dominated by Quercus suber L. considering drought scenarios. Mycorrhiza 20, 73–88.
Bahram, M., Koljalg, U., Kohout, P., Mirshahvaladi, S., Tedersoo, L., 2013. Ectomycorrhizal fungi of exotic pine plantations in relation to native host trees in Iran: evidence of host range expansion by local symbionts to distantly related host taxa. Mycorrhiza 23, 11–19.
Bourdier, T., Cordonnier, T., Kunstler, G., Piedallu, C., Lagarrigues, G., Courbaud, B., 2016. Tree size inequality reduces forest productivity: an analysis combining inventory data for ten European species and a light competition model. PLoS One 11, e0151852.
Cairney, J.W.G., 2012. Extramatrical mycelia of ectomycorrhizal fungi as moderators of carbon dynamics in forest soil. Soil Biol. Biochem. 47, 198–208.
Cheeke, T.E., Phillips, R.P., Brzostek, E.R., Rosling, A., Bever, J.D., Fransson, P., 2017. Dominant mycorrhizal association of trees alters carbon and nutrient cycling by selecting for microbial groups with distinct enzyme function. New Phytol. 214, 432–442.
Clemmensen, K.E., Finlay, R.D., Dahlberg, A., Stenlid, J., Wardle, D.A., Lindahl, B.D., 2015. Carbon sequestration is related to mycorrhizal fungal community shifts during long-term succession in boreal forests. New Phytol. 205, 1525–1536.
Coince, A., Caël, O., Bach, C., Lengellé, J., Cruaud, C., Gavory, F., et al., 2013. Below-ground fine-scale distribution and soil versus fine root detection of fungal and soil oomycete communities in a French beech forest. Fungal Ecol. 6, 223–235.
Condit, R., Engelbrecht, B.M.J., Pino, D., Pérez, R., Turner, B.L., 2013. Species distributions in response to individual soil nutrients and seasonal drought across a community of tropical trees. Proc. Natl. Acad. Sci. U. S. A. 110, 5064–5068.
Craig, M.E., Turner, B.L., Liang, C., Clay, K., Johnson, D.J., Phillips, R.P., 2018. Tree mycorrhizal type predicts within-site variability in the storage and distribution of soil organic matter. Glob. Chang. Biol. 24, 3317–3330.
Cui, L., Mu, L.Q., 2016. Ectomycorrhizal communities associated with *Tilia amurensis* trees in natural versus urban forests of Heilongjiang in Northeast China. J. For. Res. 27, 401–406.
Dolezal, J., Ishii, H., Vetrova, V.P., Sumida, A., Hara, T., 2004. Tree growth and competition in a Betula platyphylla-Larix cajanderi post-fire forest in Central Kamchatka. Ann. Bot. 94, 333–343.
Gandini, A.M.M., Grazziotti, P.H., Rossi, M.J., Grazziotti, D.C.F.S., Gandini, E.M.M., EdB, S., et al., 2015. Growth and nutrition of eucalypt rooted cuttings promoted by ectomycorrhizal fungi in commercial nurseries. Revista Brasileira de Ciência do Solo 39, 1554–1565.
Ghimire, S.R., Craven, K.D., 2011. Enhancement of switchgrass (Panicum virgatum L.) biomass production under drought conditions by the ectomycorrhizal fungus Sebacina vermifera. Appl. Environ. Microbiol. 77, 7063–7067.
Grime, J., 1998. Benefits of plant diversity to ecosystems: immediate, filter and founder effects. J. Ecol. 86, 902–910.
Hagerberg, D., Thelin, G., Wallander, H., 2003. The production of ectomycorrhizal mycelium in forests: relation between forest nutrient status and local mineral sources. Plant Soil 252, 279–290.
Hao, Z., Zhang, J., Song, B., Ye, J., Li, B., 2007. Vertical structure and spatial associations of dominant tree species in an old-growth temperate forest. For. Ecol. Manag. 252, 1–11.
Haruki, M., Tsuyuzaki, S., 2001. Woody plant establishment during the early stages of volcanic succession on Mount Usu, northern Japan. Ecol. Res. 16, 451–457.
He, Z., Xu, M., Deng, Y., Kang, S., Kellogg, L., Wu, L., et al., 2010. Metagenomic analysis reveals a marked divergence in the structure of belowground microbial communities at elevated CO2. Ecol. Lett. 13, 564–575.
Hewitt, R.E., Chapin 3rd, F.S., Hollingsworth, T.N., Taylor, D.L., 2017. The potential for mycobiont sharing between shrubs and seedlings to facilitate tree establishment after wildfire at Alaska arctic treeline. Mol. Ecol. 26, 3826–3838.
Higgins, M.A., Asner, G.P., Perez, E., Elespuru, N., Alonso, A., 2014. Variation in photosynthetic and nonphotosynthetic vegetation along edaphic and compositional gradients in northwestern Amazonia. Biogeosciences 11, 3505–3513.
Horton, T.R., Bruns, T.D., 2001. The molecular revolution in ectomycorrhizal ecology: peeking into the black-box. Mol. Ecol. 10, 1855–1871.

Jagodziński, A.M., Wierzcholska, S., Dyderski, M.K., Horodecki, P., Rusińska, A., Gdula, A.K., et al., 2018. Tree species effects on bryophyte guilds on a reclaimed post-mining site. Ecol. Eng. 110, 117–127.
Jarvis, S.G., Woodward, S., Taylor, A.F.S., 2015. Strong altitudinal partitioning in the distributions of ectomycorrhizal fungi along a short (300 m) elevation gradient. New Phytol. 206, 1145–1155.
Jia, G., Yu, X., Fan, D., Jia, J., 2016. Mechanism underlying the spatial pattern formation of dominant tree species in a natural secondary forest. PLoS One 11, e0152596.
Jonsson, L., Dahlberg, A., Nilsson, M.-C., Kårén, O., Zackrisson, O., 1999. Continuity of ectomycorrhizal fungi in self-regenerating boreal Pinus sylvestris forests studied by comparing mycobiont diversity on seedlings and mature trees. New Phytol. 142, 151–162.
Koizumi, T., Hattori, M., Nara, K., 2018. Ectomycorrhizal fungal communities in alpine relict forests of Pinus pumila on Mt. Norikura, Japan. Mycorrhiza 28, 129–145.
Krivtsov, V., Watling, R., Walker, S.J.J., Knott, D., Palfreyman, J.W., Staines, H.J., 2003. Analysis of fungal fruiting patterns at the Dawyck Botanic Garden. Ecol. Model. 170, 393–406.
Kumar, J., Atri, N.S., 2017. Studies on ectomycorrhiza: an appraisal. Bot. Rev. 84, 108–155.
Laliberté, E., Legendre, P., 2010. A distance-based framework for measuring functional diversity from multiple traits. Ecology 91, 299–305.
Lilleskov, E.A., Hobbie, E.A., Fahey, T.J., 2002. Ectomycorrhizal fungal taxa differing in response to nitrogen deposition also differ in pure culture organic nitrogen use and natural abundance of nitrogen isotopes. New Phytol. 154, 219–231.
Lilleskov, E.A., Bruns, T.D., Dawson, T.E., Camacho, F.J., 2009. Water sources and controls on water-loss rates of epigeous ectomycorrhizal fungal sporocarps during summer drought. New Phytol. 182, 483–494.
Lilleskov, E.A., Hobbie, E.A., Horton, T.R., 2011. Conservation of ectomycorrhizal fungi: exploring the linkages between functional and taxonomic responses to anthropogenic N deposition. Fungal Ecol. 4, 174–183.
Lofgren, L., Nguyen, N.H., Kennedy, P.G., 2018. Ectomycorrhizal host specificity in a changing world: can legacy effects explain anomalous current associations? New Phytol. 220, 1273–1284.
Long, D., Liu, J., Han, Q., Wang, X., Huang, J., 2016. Ectomycorrhizal fungal communities associated with Populus simonii and Pinus tabuliformis in the hilly-gully region of the Loess Plateau, China. Sci. Rep. 6, 24336.
Lopez-Zamora, I., Bliss, C., Jokela, E.J., Comerford, N.B., Grunwald, S., Barnard, E., et al., 2007. Spatial relationships between nitrogen status and pitch canker disease in slash pine planted adjacent to a poultry operation. Environ. Pollut. 147, 101–111.
Matsuoka, S., Mori, A.S., Kawaguchi, E., Hobara, S., Osono, T., 2016. Disentangling the relative importance of host tree community, abiotic environment and spatial factors on ectomycorrhizal fungal assemblages along an elevation gradient. FEMS Microbiol. Ecol. 92, fiw044.
Meier, I.C., Leuschner, C., 2014. Nutrient dynamics along a precipitation gradient in European beech forests. Biogeochemistry 120, 51–69.
Nabiollahi, K., Golmohamadi, F., Taghizadeh-Mehrjardi, R., Kerry, R., Davari, M., 2018. Assessing the effects of slope gradient and land use change on soil quality degradation through digital mapping of soil quality indices and soil loss rate. Geoderma 318, 16–28.
Nara, K., 2006a. Ectomycorrhizal networks and seedling establishment during early primary succession. New Phytol. 169, 169–178.
Nara, K., 2006b. Pioneer dwarf willow may facilitate tree succession by providing late colonizers with compatible ectomycorrhizal fungi in a primary successional volcanic desert. New Phytol. 171, 187–197.
Nara, K., Nakaya, H., Wu, B.Y., Zhou, Z.H., Hogetsu, T., 2003. Underground primary succession of ectomycorrhizal fungi in a volcanic desert on Mount Fuji. New Phytol. 159, 743–756.
Nguyen, N.H., Song, Z., Bates, S.T., Branco, S., Tedersoo, L., Menke, J., et al., 2016. FUNGuild: an open annotation tool for parsing fungal community datasets by ecological guild. Fungal Ecol. 20, 241–248.
Normand, S., Treier, U.A., Randin, C., Vittoz, P., Guisan, A., Svenning, J.-C., 2009. Importance of abiotic stress as a range-limit determinant for European plants: insights from species responses to climatic gradients. Glob. Ecol. Biogeogr. 18, 437–449.
Obase, K., Cha, J.Y., Lee, J.K., Lee, S.Y., Lee, J.H., Chun, K.W., 2009. Ectomycorrhizal fungal communities associated with Pinus thunbergii in the eastern coastal pine forests of Korea. Mycorrhiza 20, 39–49.
Ostonen, I., Helmisaari, H.-S., Borken, W., Tedersoo, L., Kukumägi, M., Bahram, M., et al., 2011. Fine root foraging strategies in Norway spruce forests across a European climate gradient. Glob. Chang. Biol. 17, 3620–3632.
Otsing, E., Barantal, S., Anslan, S., Koricheva, J., Tedersoo, L., 2018. Litter species richness and composition effects on fungal richness and community structure in decomposing foliar and root litter. Soil Biol. Biochem. 125, 328–339.
Pickles, B.J., Genney, D.R., Potts, J.M., Lennon, J.J., Anderson, I.C., Alexander, I.J., 2010. Spatial and temporal ecology of Scots pine ectomycorrhizas. New Phytol. 186, 755–768.
Põlme, S., Bahram, M., Yamanaka, T., Nara, K., Dai, Y.C., Grebenc, T., et al., 2013. Biogeography of ectomycorrhizal fungi associated with alders (Alnus spp.) in relation to biotic and abiotic variables at the global scale. New Phytol. 198, 1239–1249.
Richard, F., Millot, S., Gardes, M., Selosse, M.A., 2005. Diversity and specificity of ectomycorrhizal fungi retrieved from an old-growth Mediterranean forest dominated by Quercus ilex. New Phytol. 166, 1011–1023.
Riedler, B., Lang, S., 2018. A spatially explicit patch model of habitat quality, integrating spatio-structural indicators. Ecol. Indic. 94, 128–141.
Ruotsalainen, A.L., Markkola, A.M., Kozlov, M.V., 2009. Mycorrhizal colonisation of mountain birch (Betula pubescens ssp. czerepanovii) along three environmental gradients: does life in harsh environments alter plant-fungal relationships? Environ. Monit. Assess. 148, 215–232.
Ryberg, M., Larsson, E., Molau, U., 2009. Ectomycorrhizal diversity on Dryas octopetala and Salix reticulata in an alpine cliff ecosystem. Arct. Antarct. Alp. Res. 41, 506–514.
Sawada, Y., Aiba, S., Takyu, M., Repin, R., Nais, J., Kitayama, K., 2015. Community dynamics over 14 years along gradients of geological substrate and topography in tropical montane forests on Mount Kinabalu, Borneo. J. Trop. Ecol. 31, 117–128.
Takyu, M., Aiba, S.-I., Kitayama, K., 2002. Effects of topography on tropical lower montane forests under different geological conditions on Mount Kinabalu, Borneo. Plant Ecol. 159, 35–49.
Talbot, J.M., Bruns, T.D., Smith, D.P., Branco, S., Glassman, S.I., Erlandson, S., et al., 2013. Independent roles of ectomycorrhizal and saprotrophic communities in soil organic matter decomposition. Soil Biol. Biochem. 57, 282–291.
Taudiere, A., Munoz, F., Lesne, A., Monnet, A.C., Bellanger, J.M., Selosse, M.A., et al., 2015. Beyond ectomycorrhizal bipartite networks: projected networks demonstrate contrasted patterns between early- and late-successional plants in Corsica. Front. Plant Sci. 6, 881.
Tedersoo, L., May, T.W., Smith, M.E., 2010. Ectomycorrhizal lifestyle in fungi: global diversity, distribution, and evolution of phylogenetic lineages. Mycorrhiza 20, 217–263.
Toljander, J.F., Eberhardt, U., Toljander, Y.K., Paul, L.R., Taylor, A.F., 2006. Species composition of an ectomycorrhizal fungal community along a local nutrient gradient in a boreal forest. New Phytol. 170, 873–883.
Tuomisto, H., Ruokolainen, K., Poulsen, A.D., Moran, R.C., Quintana, C., Canas, G., et al., 2002. Distribution and diversity of pteridophytes and Melastomataceae along edaphic gradients in Yasuni National Park, Ecuadorian Amazonia. Biotropica 34, 516–533.
Tuomisto, H., Van Doninck, J., Ruokolainen, K., Moulatlet, G.M., Figueiredo, F.O.G., Siren, A., et al., 2018. Discovering floristic and geoecological gradients across Amazonia. J. Biogeogr. 46, 1734–1748.
Tuomisto, H., Van Doninck, J., Ruokolainen, K., Moulatlet, G.M., Figueiredo, F.O.G., Siren, A., et al., 2019. Discovering floristic and geoecological gradients across Amazonia. J. Biogeogr. 46, 1734–1748.
Turnbull, M.H., Goodall, R., Stewart, G.R., 1995. The impact of mycorrhizal colonization upon nitrogen source utilization and metabolism in seedlings of Eucalyptus grandis Hill ex Maiden and Eucalyptus maculata Hook. Plant, Cell and Environment 18, 1386–1394.
Turner, B.L., Hayes, P.E., Laliberté, E., 2018. A climosequence of chronosequences in southwestern Australia. Eur. J. Soil Sci. 69, 69–85.
Valverde-Barrantes, O.J., Smemo, K.A., Feinstein, L.M., Kershner, M.W., Blackwood, C.B., 2018. Patterns in spatial distribution and root trait syndromes for ecto and arbuscular mycorrhizal temperate trees in a mixed broadleaf forest. Oecologia 186, 731–741.
van der Heijden, E.W., Kuyper, T.W., 2003. Ecological strategies of ectomycorrhizal fungi of Salix repens: root manipulation versus root replacement. OIKOS 103, 668–680.
Vernes, K., Castellano, M., Johnson, C.N., 2001. Effects of season and fire on the diversity of hypogeous fungi consumed by a tropical mycophagous marsupial. J. Anim. Ecol. 70, 945–954.
Wasof, S., Lenoir, J., Gallet-Moron, E., Jamoneau, A., Brunet, J., Cousins, S.A.O., et al., 2013. Ecological niche shifts of understorey plants along a latitudinal gradient of temperate forests in north-western Europe. Glob. Ecol. Biogeogr. 22, 1130–1140.
Wen, Z., Murata, M., Xu, Z., Chen, Y., Nara, K., 2015. Ectomycorrhizal fungal communities on the endangered Chinese Douglas-fir (Pseudotsuga sinensis) indicating regional fungal sharing overrides host conservatism across geographical regions. Plant Soil 387, 189–199.
Wen, Z.G., Shi, L., Tang, Y.Z., Hong, L.Z., Xue, J.W., Xing, J.C., et al., 2018. Soil spore bank communities of ectomycorrhizal fungi in endangered Chinese Douglas-fir forests. Mycorrhiza 28, 49–58.
Wu, B.W., Gao, C., Chen, L., Buscot, F., Goldmann, K., Purahong, W., et al., 2018. Host phylogeny is a major determinant of Fagaceae-associated ectomycorrhizal fungal community assembly at a regional scale. Front. Microbiol. 9, 2409.
Yuan, Z., Gazol, A., Wang, X., Xing, D., Lin, F., Bai, X., et al., 2012. What happens below the canopy? Direct and indirect influences of the dominant species on forest vertical layers. Oikos 121, 1145–1153.
Yuan, Z.Q., Gazol, A., Lin, F., Ye, J., Shi, S., Wang, X.G., et al., 2013. Soil organic carbon in an old-growth temperate forest: spatial pattern, determinants and bias in its quantification. Geoderma 195–196, 48–55.
Yuan, Z., Gazol, A., Wang, X., Lin, F., Ye, J., Zhang, Z., et al., 2016. Pattern and dynamics of biomass stock in old growth forests: the role of habitat and tree size. Acta Oecol. 75, 15–23.
Zanne, A.E., Tank, D.C., Cornwell, W.K., Eastman, J.M., Smith, S.A., FitzJohn, R.G., et al., 2014. Three keys to the radiation of angiosperms into freezing environments. Nature 506, 89–92.
Zhang, L., Zhang, H., Wang, Z., Chen, G., Wang, L., 2016. Dynamic changes of the dominant functioning microbial community in the compost of a 90-m(3) aerobic solid state fermentor revealed by integrated meta-omics. Bioresour. Technol. 203, 1–10.